

# Wideband chaos generation without time delay signature using phase dynamics of external cavity semiconductor lasers

Anbang Wang<sup>†\*</sup>, Yuncai Wang<sup>†\*</sup> and K Alan Shore<sup>‡</sup>

<sup>†</sup>Key Laboratory of Advanced Transducers and Intelligent Control System (Taiyuan University of Technology),  
Ministry of Education and Shanxi Province

<sup>\*</sup>College of Physics and Optoelectronics, Taiyuan University of Technology  
79 West Yingze Street, Taiyuan 030024, P. R. China

<sup>‡</sup>School of Electronic Engineering, Bangor University  
Bangor, Wales LL57-1UT, UK

Email: wanganbang@tyut.edu.cn, wangyc@tyut.edu.cn, k.a.shore@bangor.ac.uk

**Abstract**—We experimentally demonstrate two methods that use phase dynamics of ECL to generate wideband chaos without signature of feedback delay: delayed self-interference and optical heterodyning. Experiments demonstrate that the incoherent delayed self-interference of an ECL can obtain chaos with about 10GHz bandwidth and  $\pm 3$ dB spectral flatness. The dominance of relaxation oscillation is cancelled and the time delay signature is suppressed. Optical heterodyning of ECLs can further enhance the bandwidth and spectral flatness, and totally eliminates the time delay signature. A wideband chaos with a colorless spectral bandwidth of 14GHz and a flatness of  $\pm 1.5$ dB is experimentally achieved. The optical heterodyning method provides an approach that generates white noise using chaos.

## 1. Introduction

Semiconductor laser with external-cavity feedback (ECL) has attracted extensive attention due to its various dynamics and applications, such as encrypted communications [1], physical random number generation [2], lidar [3], and time domain reflectometry [4]. Unfortunately, the chaotic intensity output of ECL is usually dominated by laser's relaxation oscillation [5]. Resultantly, the bandwidth is limited to several gigahertz, and then the encryption speed, the RNG generation rate and the ranging resolution are also limited. Furthermore, the ECL's intensity chaos has signature of external-cavity feedback delay [6], which means that the intensity chaos is correlated to its previous state at the feedback delay. The delay signature resultantly reduces the complexity and randomness of chaos and is therefore harmful to random number generation [2]. Moreover, the delay signature leads to security flaw because the delayed feedback system may be reconstructed if the delay time is identified [7].

Much effort has been devoted to enhancing the bandwidth of chaotic laser light or to suppressing the time-delay signature. For example, optical injection, from a chaotic laser into a static laser [8] or in opposite direction [5], has been proposed to enlarge the limited

bandwidth. The delay signature can be hidden by laser's relaxation period [9], and can be depressed by using complex feedback [10-12]. However, because their physical processes take place in laser cavity, the methods mentioned above cannot remove the dominance of laser relaxation oscillation. It is therefore interesting to establish whether an alternative method can generate a broadband chaos without signatures of relaxation oscillations and external-cavity delay.

In this paper, we demonstrate two methods that utilize the phase dynamics of ECL to generate wideband chaos, and simultaneously to flatten spectrum by eliminating the dominance of relaxation oscillation and the signature of feedback delay. The two methods are the delayed self-interference (DSI) of an ECL [13] and the optical heterodyning of two ECLs [14].

## 2. Phase dynamics of an ECL

We firstly analyze the phase dynamics of an ECL by using the Lang-Kobayashi equations [15]. The rate equations of electrical field amplitude  $A$  and phase  $\varphi$  and carrier density  $N$  are shown as follows.

$$\dot{A} = \frac{1}{2}(G - \tau_{ph}^{-1})A + \frac{\rho}{\tau_{in}}A(t - \tau)\cos\theta + \sqrt{\beta N/2\tau_N}\xi \quad (1)$$

$$\dot{\varphi} = \frac{\alpha}{2}(G - \tau_{ph}^{-1}) - \frac{\rho}{\tau_{in}}\frac{A(t - \tau)}{A}\sin\theta + \frac{1}{A}\sqrt{\beta N/2\tau_N}\zeta \quad (2)$$

$$\dot{N} = J - \tau_N^{-1}N - g(N - N_0)A^2 \quad (3)$$

where,  $G = g(N - N_0)/(1 + \varepsilon A^2)$ ,  $\theta = 2\pi\nu_0\tau + \varphi - \varphi(t - \tau)$ ,  $\tau$  is feedback delay, and  $\rho$  represents the amplitude feedback factor that indicates feedback strength as  $10\log_{10}(\rho^2)$  dB. In simulations,  $N_0 = 0.455 \times 10^6 \mu\text{m}^{-3}$  is the transparency carrier density,  $g = 1.414 \times 10^3 \mu\text{m}^3\text{ns}^{-1}$  is the differential gain,  $\varepsilon = 5 \times 10^{-5} \mu\text{m}^3$  is the gain saturation parameter,  $\tau_N = 2.5$  ns is the carrier lifetime,  $\tau_{ph} = 1.17$  ps is the photon lifetime,  $\tau_{in} = 7.38$  ps is the round-trip time in laser cavity,  $\alpha = 5.0$  is the linewidth enhancement factor,  $\beta = 10^{-3}$  is the spontaneous emission factor, and  $J_{th} = 4.239 \times 10^5 \mu\text{m}^{-3}\text{ns}^{-1}$  is the threshold current density. The last terms in equations (2) and (3) model spontaneous emission noise,

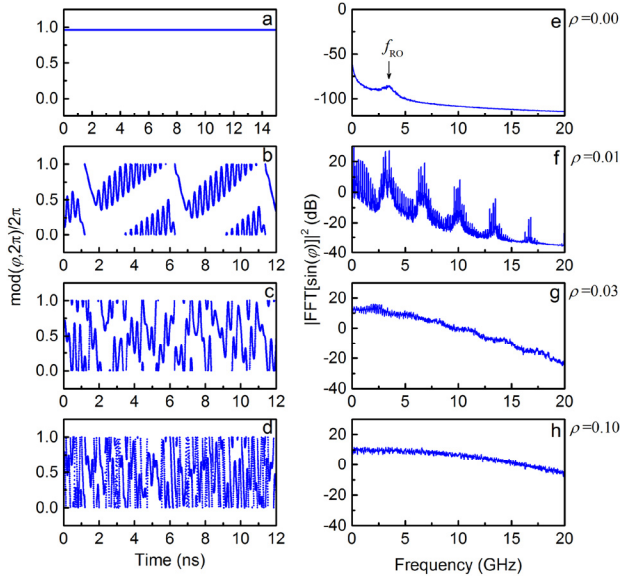


Fig. 1. Phase dynamics: (a)-(d) temporal waveforms  $\text{mod}(\varphi, 2\pi)$  and (e)-(h) corresponding spectra of  $\sin(\varphi)$  numerically obtained at feedback factors  $\rho = 0, 0.01, 0.03,$  and  $0.10,$  respectively.

where  $\xi$  and  $\zeta$  are standard normal distributed random numbers.

Figure 1 shows the phase dynamics of ECL numerically obtained with a bias current  $J = 1.8J_{th}$ , feedback delay  $\tau = 5.0$  ns, and solitary laser frequencies  $\nu_0 = 193.548$  THz. Figs. 1(a)-1(d) plot the temporal waveform of laser phase and Figs. 1(e)-1(h) display the corresponding spectra of  $\sin\varphi$  which are obtained with  $\rho = 0, 0.01, 0.03,$  and  $0.10,$  respectively. For a solitary laser, i.e.  $\rho = 0$ , the laser phase exhibits tiny and randomly fluctuation with a spectrum plotted in Fig. 1(e), which shows a relaxation-oscillation frequency of 3.5GHz. For  $\rho = 0.01$ , the laser is driven to a quasi-period state. Seen from Figs. 1(b) and 1(f), laser phase obviously presents dynamics which mainly contains the relaxation oscillation and external-cavity resonance. It is worth noting from Fig. 1(c) that, strong feedback that induces chaos leads to more complex phase dynamics; there are no clear relaxation oscillation appearing in the temporal waveform. As shown in Fig. 1(g), the spectrum of phase becomes flat and does not have a peak at the relaxation-oscillation frequency. By comparing with Fig. 1(h), one can find that further increase of feedback strength can widen and flatten the laser phase spectrum.

Therefore, delayed self-interference of an ECL and optical heterodyning of two ECLs are proposed to convert the laser phase dynamical fluctuation into intensity and then generate wideband chaos.

### 3. Delayed self-interference of an ECL

Figure 2 shows the experimental setup of the delayed self-interference. The ECL consists of a distributed feedback (DFB) semiconductor laser with optical

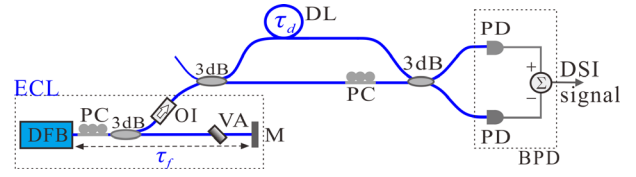


Fig. 2. Experimental setup of delayed self-interference. DL: delay line; PC: polarization controller; VA: variable attenuator; M: mirror; OI: optical isolator; PD: photodetector; BPD: balanced detector.

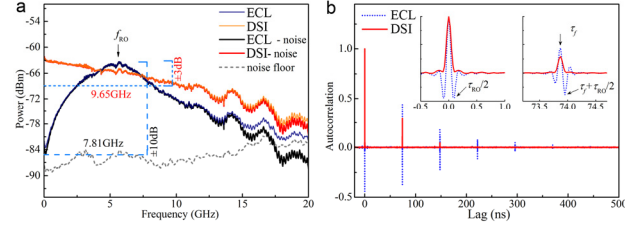


Fig. 3. (a) Experimental power spectra and (b) autocorrelation traces of chaotic ECL and its DSI signal. RBW: 1 MHz; VBW: 3 kHz. The correlation length is  $3\mu\text{s}$  which is about 40 times feedback delay.

feedback from a mirror. In the feedback path, a variable attenuator and a polarization controller are used to adjust the strength and polarization state of feedback light, respectively. After an optical isolator, the ECL output is injected into a Mach-Zehnder interferometer, in which a fiber delay line is inserted to introduce optical path difference. The delayed self-interference (DSI) signal is the difference between the two outputs of the interferometer, and is expressed as

$$I_D = A(t)A(t - \tau_d) \cos[2\pi\nu_0 t + \varphi(t) - \varphi(t - \tau_d)] \quad (4)$$

where,  $\tau_d$  is the delay corresponding to the optical path difference.

In our experiments, the DSI signal was detected by a balanced photodetector (40-GHz bandwidth, Discovery DSC-R410) that consists of two identical photodetectors and a differential amplifier. The feedback delay was 73.88 ns, and the laser was biased at 17.0 mA, which is 1.4 times the threshold current. An RF spectrum analyzer (Agilent N9020A) and a real time oscilloscope (6-GHz bandwidth, LeCroy SDA 806Zi-A) were employed to record power spectrum and time series, respectively.

Figure 3 shows an representative result of DSI. The feedback strength of the ECL is  $-13.6$  dB, and the length of the fiber delay line is 56 cm which introduces an OPD of 2.74 ns between the two arms of interferometer. Note that, the experimental feedback strength is estimated as the power ratio of the feedback light to the laser output. Figure 3(a) plots the power spectra of the ECL and its DSI signal by the blue and orange thin lines; the black and red thick curves denote the corresponding spectra after the subtraction of background noise of the spectrum analyzer. Clearly, the DSI spectrum is wider and flatter than that of the chaotic ECL. Quantitatively, we define the bandwidth as width of the band from zero to the frequency which

contains 80% of the signal energy, and the spectral flatness as the range of power fluctuation in the band. As marked in Fig. 3, the bandwidth is increased from 7.81 GHz to 9.65GHz, and the spectral flatness is greatly improved from  $\pm 10$  dB to  $\pm 3$  dB. Furthermore, the relaxation oscillation peak is erased from the power spectrum.

Figure 3(b) shows the suppression of time delay signature by autocorrelation function (ACF). As plotted in the dotted line, the ACF trace of ECL has five peaks separately at  $\tau_f$ ,  $2\tau_f$ ,  $3\tau_f$ ,  $4\tau_f$ , and  $5\tau_f$  with gradually reduced height. In comparison, the ACF trace of the DSI signal has only two shortened peaks at  $\tau_f$  and  $2\tau_f$ , depicted by the solid line. This means the time-delay signature is depressed. In addition, as shown in the left inset, the ACF trace of the DSI signal also has no obvious valley at about  $\tau_{RO}/2$ , that means the relaxation oscillation signature is dispelled.

#### 4. Optical Heterodyning of ECLs

Note that the DSI signal has a downward-sloping spectrum with a small bandwidth and still has the time delay signature. In this section, we demonstrate that optical heterodyning method can further enhance bandwidth and eliminate the signatures feedback delay.

Figure 4 presents the experimental arrangement of the optical heterodyning method. Each ECL that is shown in the dashed box consists of a DFB semiconductor laser subject to optical feedback from a fiber mirror. The feedback delay time of ECL<sub>1</sub> and ECL<sub>2</sub> are denoted as  $\tau_1$  and  $\tau_2$ , respectively. The two delays are taken to be incommensurate,  $q\tau_1 \neq p\tau_2$ , for any positive integers  $q$  and  $p$ . The outputs of the two ECLs are coupled through a 3-dB fiber coupler, and their heterodyne signal is subsequently extracted by a balanced detector. In principle, the heterodyne signal is expressed as

$$I_H = 2A_1A_2 \cos[2\pi\Delta\nu_0 t + \varphi_2(t) - \varphi_1(t)] \quad (5)$$

where  $\nu_{01}$ ,  $\nu_{02}$  are the solitary frequencies of two lasers, and  $\Delta\nu_0 = \nu_{02} - \nu_{01}$  is frequency detuning.

In experiments, the lasers DFB<sub>1</sub> and DFB<sub>2</sub> (WTD LDM5S752) have threshold values of 10.3 mA and 11.0mA, respectively, and both are biased at 14.8 mA by laser drivers. The lasers' wavelengths are stabilized and tuned by temperature controllers. The two feedback delays are  $\tau_1 = 85.3$  ns and  $\tau_2 = 110.7$  ns, respectively. A fast balanced photodetector with a bandwidth of 40GHz (Discovery DSC R410) is used to extract the heterodyne signal. An optical tunable delay line (General Photonics, MDL-002) that has a resolution of less than 0.3 $\mu$ m is used to minimize the optical path difference between the two fiber paths before the balanced detector.

Figure 5 presents the representative results that are obtained with the following parameters, feedback strengths  $\kappa_1 = -15.9$  dB and  $\kappa_2 = -19.5$  dB and the lasers' center wavelengths  $\lambda_1 = 1549.980$  nm and  $\lambda_2 = 1549.882$  nm.

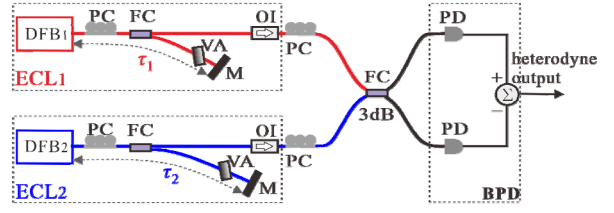


Fig. 4. Experimental setup of optical heterodyning method. PC: polarization controller; FC: fiber coupler; OC: optical circulator; VA: variable optical attenuator; M: mirror; OI: optical isolator; PD: photodetector; BPD: balanced detector.

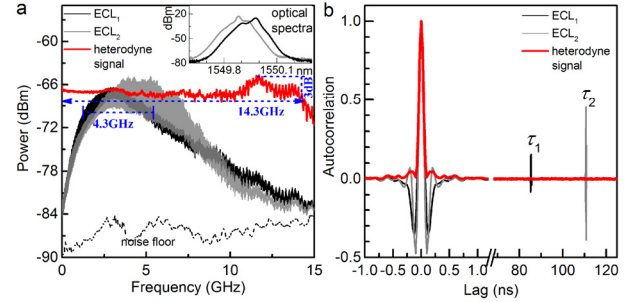


Fig. 5. (a) Experimental power spectra and (b) autocorrelation traces of chaotic ECL and its DSI signal. RBW: 1 MHz; VBW: 3 kHz. The correlation length is  $3\mu$ s which is about 40 times feedback delay.

Figure 5(a) shows the spectrum of the heterodyne signal as the gray (red) line as well as the spectra of the intensity chaos of ECL<sub>1</sub> and ECL<sub>2</sub> as the black and light gray lines, respectively. One can find from the black or light gray lines that the spectrum of laser intensity chaos covers a wide frequency range of 15GHz. However, it has an obvious peak approximately at the laser relaxation frequency, the peak being approximately 18 dB higher than the lowest spectral component. That is, the whole spectrum is dominated by the relaxation oscillation frequency. By contrast, the RF spectrum of the optical heterodyne signal is very flat over a wide frequency band and is free of dominant peaks. Specifically, the spectrum is contained with a power range of 3 dB for frequencies up to 14.3 GHz. It is worth noting that the 3-dB bandwidth of 14.3 GHz exceeds that of some reported amplified spontaneous emission lights [16].

Figure 5(b) plots the corresponding ACF traces, which are calculated with time series recorded by a 6-GHz real-time oscilloscope. Shown as the black and light gray lines, the ACF traces of ECLs exhibit obvious relaxation oscillation after the main peak at zero lag. Additionally, each correlation trace has a distinct peak at the feedback delay, i.e.,  $ACF_1(\tau_1) = 0.155$  and  $ACF_2(\tau_2) = 0.416$ . By contrast, the ACF trace of the heterodyne signal shown as the gray (red) line does not have peaks at the two delays: the correlation values at  $\tau_1$  and  $\tau_2$  are  $-2.5 \times 10^{-4}$  and  $1.2 \times 10^{-4}$ , less than the standard deviation of  $1.14 \times 10^{-3}$  of the background noise. Furthermore, the ACF trace does

not have obvious relaxation oscillation like that of laser intensity chaos. These mean that the optical heterodyning simultaneously eliminates signatures of feedback delay and relaxation oscillation.

The elimination of the feedback delay signature is attributed to the non-resonant beatings between two sets of external-cavity modes (ECMs) with different frequency spans. The reason of the signature appearing in intensity chaos is understood as follows: Laser intensity is measured by square-law detection of optical field and thus consists of beats among ECMs, for instance,  $\nu_p = p/\tau_1$  for ECL<sub>1</sub>; all the beats are resonant at frequencies of  $f_m = m/\tau_1$ , leading to period in chaos. For the heterodyne signal, there is only the beating between two laser fields. Considering the ECMs of ECL<sub>1</sub> and ECL<sub>2</sub> as  $\nu_p = p/\tau_1$  and  $\nu_q = q/\tau_2$ , respectively, we can deduce the beat frequencies as  $f_{pq} = p/\tau_1 - q/\tau_2$ . For arbitrary integer pairs ( $p, q$ ) and ( $p', q'$ ), one can get  $f_{pq} \neq f_{p'q'}$  under the condition of that the two delays are incommensurate. This means that all of the beat frequencies between the two sets of ECMs are different or non-resonant. There is therefore no external-cavity resonance or feedback delay signature in the heterodyne signal.

We mention that both DSI and optical heterodyning can improve the symmetry of probability distribution. The skewness is decreased by more than one order of magnitude, which is beneficial to achieving nearly equal numbers of ones and zeros in random number generation.

## 5. Conclusions

In summary, we have proposed two approaches, delayed self-interference and optical heterodyning, to generate wideband chaos. Experiments demonstrate that the DSI method can obtain chaos with about 10GHz bandwidth and  $\pm 3$ dB spectral flatness. The dominance of relaxation oscillation is eliminated and the time delay signature is suppressed. Optical heterodyning further enhances the bandwidth and spectral flatness, and totally eliminates the time delay signature. A colorless spectrum with 14GHz bandwidth and  $\pm 1.5$ dB flatness is experimentally achieved, which indicates an alternative method to generate white noise using chaos [17].

## Acknowledgments

This work was supported in part by the NSFC under Grants 61227016 and 61475111, in part by the International Science and Technology Cooperation Program of China under Grant 2014DFA50870, in part by the Program for the Innovative Talents of Higher Learning Institutions of Shanxi, in part by the Natural Science Foundation for Excellent Young Scientists of Shanxi Province under Grant 2015021004, and in part by the Program for Excellent Talents in Taiyuan University of Technology under Grant 2014YQ001.

## References

- [1] A. Argyris *et al*, "Chaos-based communications at high bit rates using commercial fibre-optic links," *Nature* vol.438, pp.343-346, 2005.
- [2] A. Uchida *et al*, "Fast physical random bit generation with chaotic semiconductor lasers," *Nat. Photon.*, Vol.2, pp.728-732, 2008.
- [3] F. Y. Lin *et al*, "Chaotic lidar," *IEEE J. Sel. Topics Quantum Electron.*, vol. 10, pp. 991-997, 2004.
- [4] Y. C. Wang *et al*, "Chaotic correlation optical time domain reflectometer utilizing laser diode," *IEEE Photon. Technol. Lett.*, vol. 20, pp.1636-1638, 2008.
- [5] A. B. Wang *et al*, "Enhancing the bandwidth of the optical chaotic signal generated by a semiconductor Laser with optical feedback," *IEEE Photon. Technol. Lett.*, vol.20, pp.1633-1635, 2008.
- [6] D. Rontani *et al*, "Time-delay identification in a chaotic semiconductor laser with optical feedback: a dynamical point of view," *IEEE J. Quantum Electron.*, vol.45, pp.879-891, 2009.
- [7] R. Hegger *et al*, "Identifying and modeling delay feedback systems," *Phys. Rev. Lett.*, vol.81, pp.558-561, 1998.
- [8] A. Uchida *et al*, "High-frequency broadband signal generation using a semiconductor laser with a chaotic optical injection," *IEEE J. Quantum Electron.*, vol. 39, pp. 1462-1467, 2003.
- [9] D. Rontani *et al*, "Loss of time-delay signature in the chaotic output of a semiconductor laser with optical feedback," *Opt. Lett.*, vol.32, pp. 2960-2962, 2007.
- [10] J.-G. Wu *et al*, "Suppression of time delay signatures of chaotic output in a semiconductor laser with double optical feedback," *Opt. Express*, vol.017, pp.20124-20133, 2009.
- [11] N. Oliver *et al*, "Dynamics of a semiconductor laser with polarization-rotated feedback and its utilization for random bit generation," *Opt. Lett.*, vol.36, pp. 4632-4634, 2011.
- [12] S.-S. Li and S.-C. Chan, "Chaotic Time-Delay Signature Suppression in a Semiconductor Laser With Frequency-Detuned Grating Feedback," *IEEE J. Sel. Topics Quantum Electron.*, vol. 21, pp. 1800812, 2015
- [13] A. B. Wang *et al*, "Generation of wide chaos with suppressed time-delay signature by delayed self-interference," *Opt. Express*, vol.21, pp.8701-8710, 2013
- [14] A. B. Wang *et al*, "Optical Heterodyne Generation of High-Dimensional and Broadband White Chaos," *IEEE J. Sel. Topics Quantum Electron.*, vol. 21, pp. 1800710, 2015
- [15] R. Lang and K. Kobayashi, "External optical feedback effects on semiconductor injection laser properties," *IEEE J. Quantum Electron.*, vol.16, pp.347-355, 1980.
- [16] C. R. Williams *et al*, "Fast physical random number generator using amplified spontaneous emission," *Opt. Express*, vol. 18, pp. 23584- 23597, 2010.
- [17] R. L. Kautz, "Using chaos to generate white noise," *J. Appl. Phys.*, vol. 86, pp. 5794-5800, 1999.